Reactions of Ruthenium(II)-co-ordinated Phenyl Phosphines: Synthesis and X-Ray Crystal Structures of the Orthometallated Complexes $[Ru(C_6H_4PR^1R^2)(CH_2SiMe_3)(\eta^6\text{-}C_6Me_6)]$ ($R^1 = R^2 = Ph$; $R^1 = Ph$, $R^2 = Me$; $R^1 = R^2 = Me$) and of $[\{Ru(CH_2SiMe_3)_2(\mu\text{-}\sigma,\eta^6\text{-}PMe_2Ph)\}_2]$ containing Bridging Dimethylphenylphosphine Ligands *

Pietro Diversi, Giovanni Ingrosso, Antonio Lucherini, and Fabio Marchetti
Dipartimento di Chimica e Chimica Industriale, Università di Pisa, Via Risorgimento 35, 56100 Pisa, Italy
Victor Adovasio and Mario Nardelli
Istituto di Chimica Generale ed Inorganica dell'Università di Parma, Centro di Studio per la Strutturistica Diffrattometrica del CNR, Viale delle Scienze, 43100 Parma, Italy

The compounds $[RuCl_2(\eta^6\text{-}C_6Me_6)L]$ [L = PPh_3, (**1**); $PMePh_2$, (**2**); or PMe_2Ph, (**3**)] react with an excess of $Mg(CH_2SiMe_3)Cl$ to give the corresponding orthometallated complexes $[Ru(C_6H_4PR^1R^2)(CH_2SiMe_3)(\eta^6\text{-}C_6Me_6)]$ [$R^1 = R^2 = Ph$, (**4**); $R^1 = Ph$, $R^2 = Me$, (**5**); $R^1 = R^2 = Me$, (**6**)]. Both diastereomers of (**5**) have been isolated in a pure form. In the alkylation of (**3**) the dimeric dialkyl derivative $[\{Ru(CH_2SiMe_3)_2(\mu\text{-}\sigma,\eta^6\text{-}PMe_2Ph)\}_2]$ (**7**) and the chloroalkyl compound $[RuCl(CH_2SiMe_3)(\eta^6\text{-}C_6Me_6)(PMe_2Ph)]$ (**8**) have also been isolated. The *X*-ray crystal structures of complexes (**4**)—(**7**) have been determined. Crystal data are: (**4**), *a* = 10.622(3), *b* = 15.851(10), *c* = 18.963(18) Å, β = 103.64(2)°, *Z* = 4, space group $P2_1/c$, *R* (2 202 reflections, 506 parameters) = 0.0599; (**5a**), *a* = 12.215(8), *b* = 17.920(10), *c* = 13.023(7) Å, β = 100.02(2)°, *Z* = 4, space group $P2_1/a$, *R* (4 505, 453) = 0.0528; (**5b**), *a* = 11.457(6), *b* = 11.452(5), *c* = 10.736(5) Å, α = 91.96(1), β = 96.39(1), γ = 87.92(1)°, *Z* = 2, space group $P\bar{1}$, *R* (5 855, 453) = 0.0435; (**6**), *a* = 14.633(4), *b* = 14.527(4), *c* = 11.936(3) Å, α = 94.03(1), β = 91.54(1), γ = 77.78(1)°, *Z* = 4, space group $P\bar{1}$, *R* (5 763, 244) = 0.0393; (**7**), *a* = 15.966(2), *b* = 13.165(1), *c* = 21.213(5) Å, β = 109.94(1), *Z* = 8, space group *C*2/*c*, *R* (2 899, 191) = 0.0593. The molecular structures of (**4**)—(**6**) are of the 'three-legged piano-stool' type, where the bulky C_6Me_6 ligand (effective cone angle 157—160°) produces widenings of the other co-ordination polyhedron angles. The orthometallated ring is planar and practically coplanar with the benzene ring that shows significant deformations in the angles at the carbon atoms involved in the cyclometallation. The molecular structure of complex (**7**) is binuclear with a centrosymmetric six-membered ring having a chair conformation. The formation of the orthometallated compounds is discussed.

Cyclometallation reactions involving intramolecular C–H activation of hydrocarbyl ligands have recently attracted great interest since the discovery that some transition-metal centres insert into C–H bonds of alkanes.[1,2] In this context we have recently studied the alkylation reactions of rhodium(III) and iridium(III) systems $[MCl_2(\eta^5\text{-}C_5Me_5)(PPh_3)]$ (M = Rh or Ir) with neopentyl and trimethylsilylmethyl alkylating agents: dialkyl derivatives, or cyclometallation products of the alkyl or the triphenylphosphine ligand, *i.e.* metallacyclobutanes or orthometallated alkyl complexes, are formed depending on the experimental conditions. For instance, reaction of $[RhCl_2(\eta^5\text{-}C_5Me_5)(PPh_3)]$ with $Mg(CH_2EMe_3)Cl$ (E = C or Si) gives the rhodacyclobutane $[Rh(CH_2CMe_2CH_2)(\eta^5\text{-}C_5Me_5)(PPh_3)]$ or the dialkyl complex $[Rh(CH_2SiMe_3)_2(\eta^5\text{-}C_5Me_5)(PPh_3)]$ respectively, while treatment with $Li(CH_2EMe_3)$ gives the orthometallated complex $[Rh(C_6H_4PPh_2)(CH_2EMe_3)(\eta^5\text{-}C_5Me_5)]$.[3]

We have now turned our attention to the reactions of the isoelectronic ruthenium(II) systems $[RuCl_2(\eta^6\text{-}C_6Me_6)L]$ (L = PPh_3, $PMePh_2$, or PMe_2Ph) with $Mg(CH_2EMe_3)Cl$ (E = C or Si). We describe here the orthometallation reactions which have been observed in the alkylation of the above ruthenium compounds with the trimethylsilylmethyl Grignard reagent, and the isolation of the dimeric dialkyl complex $[\{Ru(CH_2SiMe_3)_2(\mu\text{-}\sigma,\eta^6\text{-}PMe_2Ph)\}_2]$ with the σ,η^6-phosphine ligand bridging two ruthenium atoms in a six-membered ring. A preliminary account of this research has been communicated.[4]

Results and Discussion

Reaction of $[RuCl_2(\eta^6\text{-}C_6Me_6)L]$ [L = PPh_3, (**1**); $PMePh_2$, (**2**); *or* PMe_2Ph, (**3**)] *with* $Mg(CH_2SiMe_3)Cl$.—Treatment of complexes (**1**) and (**2**) with an excess of $Mg(CH_2SiMe_3)Cl$ in pentane at room temperature followed by hydrolysis at 0 °C, and purification by column chromatography, yields orange crystals of the corresponding trimethylsilylmethyl derivatives of ruthenium(II), (**4**) and (**5**), containing orthometallated phosphines (Scheme). In the case of (**5**) both ruthenium and phosphorus are chiral centres, so that a pair of diastereomers, (**5a**) and (**5b**), can exist. The ^1H n.m.r. spectrum of the hydrolyzed reaction mixture shows that the two diastereomers are formed in different amounts [(**5a**)/(**5b**) = 2:1] (see the crystallographic section for comments). The two diastereomers have been separated by column chromatography on alumina: elution with pentane gives (**5a**), then pentane–diethyl ether (3:1) elutes (**5b**).

---

* (*o*-Diphenylphosphinophenyl-C^1P)(η^6-hexamethylbenzene)(trimethylsilylmethyl)ruthenium(II), (*RR*:*SS*)- and (*RS*:*SR*)-(η^6-hexamethylbenzene)(*o*-methylphenylphosphinophenyl-C^1P)(trimethylsilylmethyl)ruthenium(II), (*o*-dimethylphosphinophenyl-C^1P)(η^6-hexamethylbenzene)(trimethylsilylmethyl)ruthenium(II), and bis(μ-dimethylphosphinobenzene-$C^{1-6}P$)-bis[bis(trimethylsilylmethyl)-ruthenium(II)].

Supplementary data available: see Instructions for Authors, *J. Chem. Soc., Dalton Trans.*, 1990, Issue 1, pp. xix—xxii.

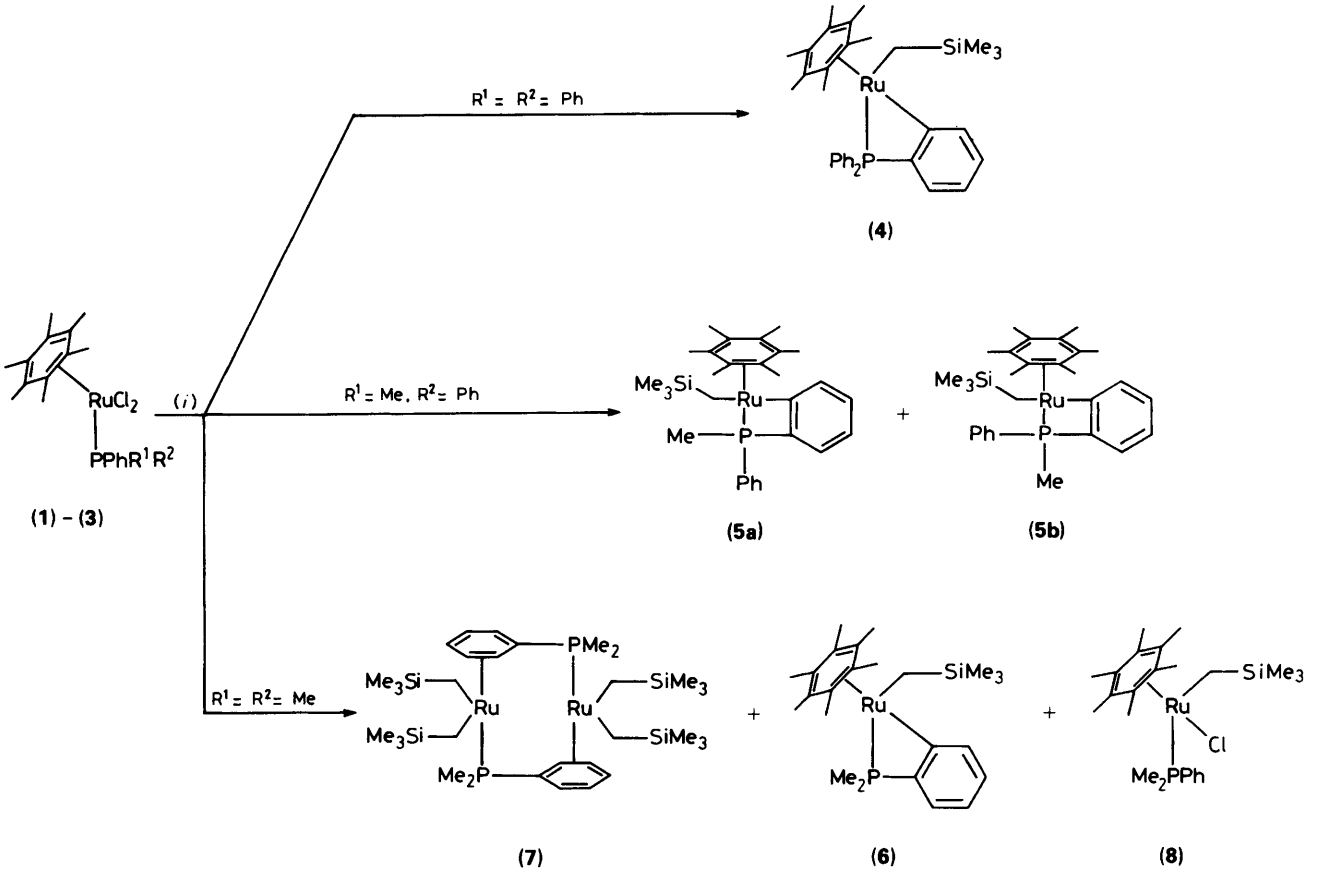

Scheme. (*i*) $Mg(CH_2SiMe_3)Cl$, pentane, 20 °C

Treatment of complex (**3**) with an excess of $Mg(CH_2SiMe_3)Cl$ in pentane at room temperature followed by hydrolysis gives a mixture of several organometallic compounds. By column chromatography separation three major products have been isolated: a dialkyl derivative containing the bridging σ,η^6-PMe_2Ph ligand $[\{Ru(CH_2SiMe_3)_2(\mu\text{-}\sigma,\eta^6\text{-}PMe_2Ph)\}_2]$ (**7**) (pentane as eluant), the orthometallated compound $[Ru(C_6H_4PMe_2)(CH_2SiMe_3)(\eta^6\text{-}C_6Me_6)]$ (**6**) [pentane–diethyl ether (5:1)], and the chloroalkyl compound $[RuCl(CH_2SiMe_3)(\eta^6\text{-}C_6Me_6)(PMe_2Ph)]$ (**8**) [pentane–diethyl ether (1:1)] (Scheme). Compound (**8**) decomposes in part during the chromatographic purification on alumina and it is more conveniently prepared by changing the alkylation procedure ([Mg]/[Ru] molar ratio 1.5:1, diethyl ether as the solvent, addition of dioxane). Under these conditions (**8**) is formed as the only product and it has been isolated in 55% yield by crystallization from pentane. Compounds (**6**)—(**8**) are not the only products of the alkylation of (**3**) with an excess of alkylating agent: indeed the ^1H n.m.r. analysis of the hydrolyzed reaction mixture shows the presence of at least two other organometallic compounds which are lost in the further work-up.

We have also attempted the alkylation of $[RuCl_2(\eta^6\text{-}C_6Me_6)(PEt_3)]$ with $Mg(CH_2SiMe_3)Cl$ and $Li(CH_2SiMe_3)$ in order to know whether the presence of an entirely aliphatic trialkylphosphine could influence in some way the course of the reaction: however we have not been able to isolate any organometallic compound owing to the extensive decomposition of the reaction mixture during attempted purification.

Finally the use of $Li(CH_2SiMe_3)$, instead of the Grignard reagent, in the alkylation of (**1**)—(**3**) does not lead to the isolation of any product.

Analytical and ^1H n.m.r. data for the new complexes (**4**)—(**8**) are reported in Table 1. All the orthometallated compounds (**4**)—(**6**) give well resolved ^1H n.m.r. spectra, whose main features are the non-equivalence of the methylene protons in the CH_2SiMe_3 group and a characteristic pattern of four multiplets in the region δ 6.5—7.5, due to the aromatic protons of the orthometallated benzene ring. The ^1H n.m.r. spectrum of (**7**) is characterized by the presence of three multiplets in the region δ 4.8—5.7, due to the protons of the η^6-bonded phenyl group of the phosphine.

The orthometallated derivative (**6**) can be also prepared by treating (**8**) with $Mg(CH_2SiMe_3)Cl$, the yield being approximately the same as that observed in the alkylation of the dichloro compound (**3**).

We have tried to carry out the reaction (**8**) $\longrightarrow$ (**6**), which is formally a deprotonation reaction, by using as the alkylating agents MgMeI and LiMe, but in the case of MgMeI we did not observe any reaction at all and with LiMe a simple alkylation occurred to give the dialkyl derivative $[RuMe(CH_2SiMe)(\eta^6\text{-}C_6Me_6)(PMe_2Ph)]$ (**9**) (Table 1).

Crystal Structure Analysis of Compounds (**4**), (**5a**), (**5b**), (**6**), *and* (**7**).—The final atomic co-ordinates of the non-hydrogen atoms of compounds (**4**)—(**7**) are quoted in Table 2, and the relevant structural parameters for the orthometallated complexes are compared in Table 3. The thermal-motion analyses were carried out in Schomaker and Trueblood's[5] rigid-body approximation considering also the internal motions of some groups according to Dunitz and White's one-parameter model.[6,7] This analysis was considered also for the non-disordered part of compound (**7**).

The major discrepancies are found for the hexamethylbenzene methyl groups and for some carbon atoms of the non-orthometallated phenyl groups, which execute large-amplitude

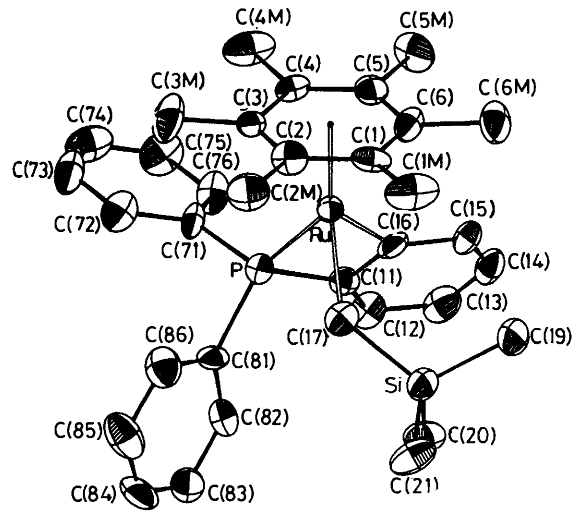

(4)

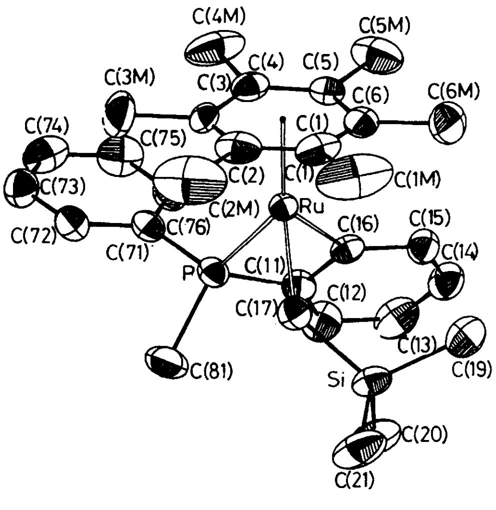

(5a)

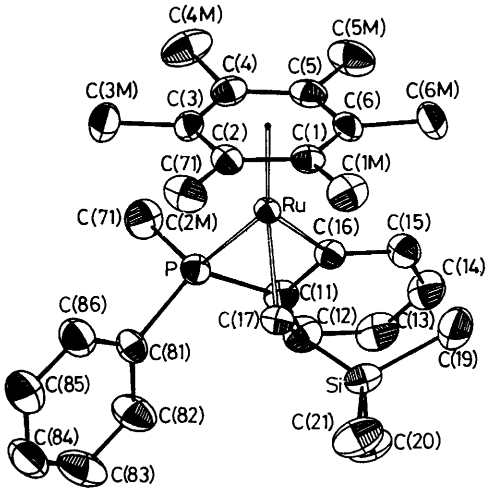

(5b)

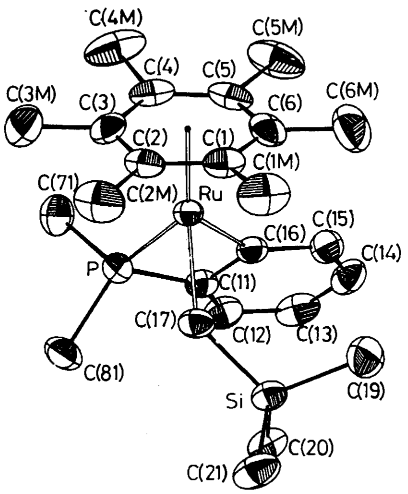

(6) Molecule A

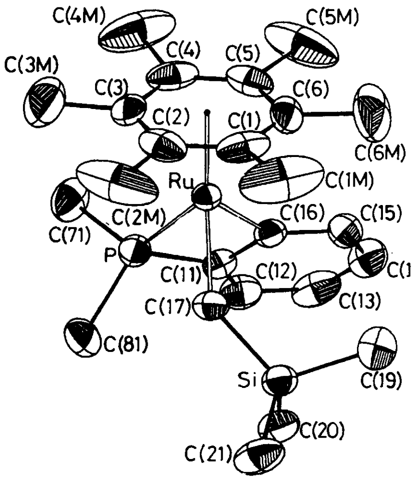

(6) Molecule B

Figure 1. ORTEP drawings of the complexes (**4**), (**5a**), (**5b**), and (**6**) showing the molecular structure and thermal motion. The hydrogen atoms are omitted for clarity. Thermal ellipsoids are at 40% probability

Table 1. Analytical and spectroscopic data

Compound, colour, and analysis[a]	^{1}H N.m.r. data[b]
(4) $[\mathrm{Ru}(o\text{-}\mathrm{C_6H_4PPh_2})(\mathrm{CH_2SiMe_3})(\eta^6\text{-}\mathrm{C_6Me_6})]$ Orange-yellow C, 66.90 (66.75); H, 7.15 (7.10) 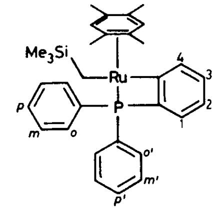	−0.37 [1 H, dd, J(H–H) 12.8, J(H–P) 15.7, CHSi], −0.17 (9 H, s, $\mathrm{SiMe_3}$), 0.17 [1 H, dd, J(H–H) 12.8, J(H–P) 1.5, CHSi], 1.72 [18 H, d, J(H–P) 0.5, $\mathrm{C_6Me_6}$], 6.70—6.96 (4 H, m, $\mathrm{H^1 + H_{m'} + H_{p'}}$), 6.98—7.20 (6 H, m, $\mathrm{H^2 + H_m + H_p + H_{o'}}$), 7.31 [1 H, dt, $J(\mathrm{H^2–H^3}) \approx J(\mathrm{H^3–H^4})$ 7.3, $J(\mathrm{H^3–H^1})$ 1.5, $\mathrm{H^3}$], 7.57 [1 H, dd, $J(\mathrm{H^4–H^3})$ 7.3, J(H–P) 4.3, $\mathrm{H^4}$], 7.66 [2 H, ddd, $J(\mathrm{H_o–H_m})$ 9.5, $J(\mathrm{H_o–H_p})$ 1.5, J(H–P) 8.1, $\mathrm{H_o}$]
(5a) (*RR*:*SS*) $[\mathrm{Ru}(o\text{-}\mathrm{C_6H_4PMePh})(\mathrm{CH_2SiMe_3})(\eta^6\text{-}\mathrm{C_6Me_6})]$[c] Orange-yellow C, 64.10 (63.35); H, 7.40 (7.50) 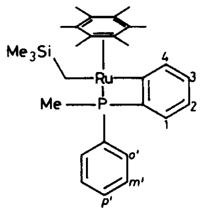	0.02 [1 H, dd, J(H–H) 13.2, J(H–P) 15.6, CHSi], 0.04 (9 H, s, $\mathrm{SiMe_3}$), 0.16 [1 H, dd, J(H–H) 13.2, J(H–P) 2.9, CHSi], 1.55 [3 H, d, J(H–P) 9.6, PMe], 1.64 [18 H, d, J(H–P) 0.8, $\mathrm{C_6Me_6}$], 6.55 [1 H, ddd, $J(\mathrm{H^1–H^2})$ 7.4, $J(\mathrm{H^1–H^3})$ 1.2, J(H–P) 11.5, $\mathrm{H^1}$], 6.95 [1 H, ddt, $J(\mathrm{H^2–H^1}) \approx J(\mathrm{H^2–H^3})$ 7.4, $J(\mathrm{H^2–H^4})$ 1.1, J(H–P) 2.9, $\mathrm{H^2}$], 6.97—7.04 (3 H, m, $\mathrm{H_{m'} + H_{p'}}$), 7.14—7.22 (2 H, m, $\mathrm{H_{o'}}$), 7.27 [1 H, dt, $J(\mathrm{H^3–H^2}) \approx J(\mathrm{H^3–H^4})$ 7.4, $J(\mathrm{H^3–H^1})$ 1.4, $\mathrm{H^3}$], 7.53 [1 H, dd, $J(\mathrm{H^4–H^3})$ 7.4, J(H–P) 4.3, $\mathrm{H^4}$]
(5b) (*RS*:*SR*) $[\mathrm{Ru}(o\text{-}\mathrm{C_6H_4PMePh})(\mathrm{CH_2SiMe_3})(\eta^6\text{-}\mathrm{C_6Me_6})]$[c] Orange-yellow C, 63.70 (63.35); H, 7.60 (7.50) 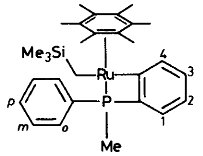	−0.72 [1 H, dd, J(H–H) 13.1, J(H–P) 17.1, CHSi], −0.15 (9 H, s, $\mathrm{SiMe_3}$), 0.06 [1 H, dd, J(H–H) 13.1, J(H–P) 1.3, CHSi], 1.37 [3 H, d, J(H–P) 9.3, PMe], 1.86 [18 H, d, J(H–P) 0.8, $\mathrm{C_6Me_6}$], 6.84 [1 H, ddd, $J(\mathrm{H^1–H^2})$ 7.3, $J(\mathrm{H^1–H^3})$ 1.5, J(H–P) 11.3, $\mathrm{H^1}$], 6.96 [1 H, ddt, $J(\mathrm{H^2–H^3}) \approx J(\mathrm{H^2–H^1})$ 7.3, $J(\mathrm{H^2–H^4})$ 1.1, J(H–P) 3.3, $\mathrm{H^2}$], 7.02—7.20 (3 H, m, $\mathrm{H_m + H_p}$), 7.26 [1 H, dt, $J(\mathrm{H^3–H^2}) \approx J(\mathrm{H^3–H^4})$ 7.3, $J(\mathrm{H^3–H^1})$ 1.5, $\mathrm{H^3}$], 7.51 [2 H, ddd, $J(\mathrm{H_o–H_m})$ 9.8, $J(\mathrm{H_o–H_p})$ 1.5, J(H–P) 8.2, $\mathrm{H_o}$], 7.45—7.56 (1 H, m, obscured, $\mathrm{H^4}$)
(6) $[\mathrm{Ru}(o\text{-}\mathrm{C_6H_4PMe_2})(\mathrm{CH_2SiMe_3})(\eta^6\text{-}\mathrm{C_6Me_6})]$ Orange-yellow C, 59.85 (59.10); H, 8.15 (8.05) 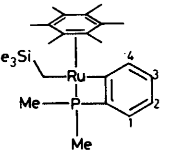	−0.22 [1 H, dd, J(H–H) 13.1, J(H–P) 16.6, CHSi], −0.03 (9 H, s, $\mathrm{SiMe_3}$), 0.07 [1 H, dd, J(H–H) 13.1, J(H–P) 2.2, CHSi], 1.11 [3 H, d, J(H–P) 9.2, PMe], 1.18 [3 H, d, J(H–P) 9.5, PMe], 1.79 [18 H, d, J(H–P) 0.8, $\mathrm{C_6Me_6}$], 6.50 [1 H, dddd, $J(\mathrm{H^1–H^2})$ 7.3, $J(\mathrm{H^1–H^3})$ 1.4, $J(\mathrm{H^1–H^4})$ 0.8, J(H–P) 12.4, $\mathrm{H^1}$], 6.89 [1 H, ddt, $J(\mathrm{H^2–H^3}) \approx J(\mathrm{H^2–H^1})$ 7.4, $J(\mathrm{H^2–H^4})$ 1.1, J(H–P) 2.9, $\mathrm{H^2}$], 7.21 [1 H, dt, $J(\mathrm{H^3–H^4}) \approx J(\mathrm{H^3–H^2})$ 7.4, $J(\mathrm{H^3–H^1})$ 1.4, $\mathrm{H^3}$], 7.43 [1 H, ddt, $J(\mathrm{H^4–H^3})$ 7.33, $J(\mathrm{H^4–H^2}) \approx J(\mathrm{H^4–H^1})$ 0.9, J(H–P) 4.0, $\mathrm{H^4}$]
(7) $[\{\mathrm{Ru}(\mathrm{CH_2SiMe_3})_2(\mu\text{-}\sigma,\eta^6\text{-}\mathrm{PMe_2Ph})\}_2]$ Orange-yellow C, 46.90 (46.45); H, 8.10 (8.05) 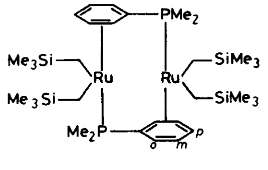	−0.48 [1 H, dd, J(H–H) 12.9, J(H–P) 6.9, CHSi], −0.41 [1 H, dd, J(H–H) 12.9, J(H–P) 10.1, CHSi], 0.29 (18 H, s, $\mathrm{SiMe_3}$), 1.09 [6 H, d, J(H–P) 8.5, $\mathrm{PMe_2}$], 4.89 [2 H, t, $J(\mathrm{H_m–H_o}) \approx J(\mathrm{H_m–H_p})$ 5.8, $\mathrm{H_m}$], 5.44—5.49 (2 H, m, $\mathrm{H_o}$), 5.66 [1 H, dt, $J(\mathrm{H_p–H_m})$ 5.7, J(H–P) 1.7, $\mathrm{H_p}$]
(8) $[\mathrm{RuCl}(\mathrm{CH_2SiMe_3})(\eta^6\text{-}\mathrm{C_6Me_6})(\mathrm{PMe_2Ph})]$ Orange C, 55.25 (55.00); H, 7.70 (7.70); Cl, 6.60 (6.75) 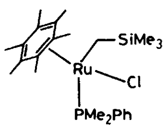	−0.29 [1 H, dd, J(H–H) 13.1, J(H–P) 16.6, CHSi], 0.56 (9 H, s, $\mathrm{SiMe_3}$), 0.63 [1 H, d, J(H–H) 13.1, CHSi], 1.13 [3 H, d, J(H–P) 8.7, PMe], 1.47 [18 H, d, J(H–P) 0.7, $\mathrm{C_6Me_6}$], 1.56 [3 H, d, J(H–P) 9.8, PMe], 7.02—7.16 (3 H, m, $\mathrm{H_p + H_m}$), 7.70 [2 H, ddd, $J(\mathrm{H_o–H_m})$ 9.6, $J(\mathrm{H_o–H_p})$ 1.7, J(H–P) 7.8, $\mathrm{H_o}$]

Table 1 (*continued*)

(**9**) $[RuMe(CH_2SiMe_3)(\eta^6\text{-}C_6Me_6)(PMe_2Ph)]$ Yellow C, 59.75 (59.60); H, 8.65 (8.60)		
	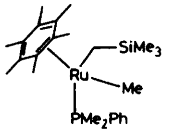	−0.56 [1 H, t, *J*(H–H) ≈ *J*(H–P) 13.0, CHSi], −0.30 [1 H, dd, *J*(H–H) 13.0, *J*(H–P) 1.4, CHSi], 0.24 [3 H, d, *J*(H–P) 6.8, RuMe], 0.36 (9 H, s, $SiMe_3$), 1.22 [3 H, d, *J*(H–P) 8.3, PMe], 1.30 [3 H, d, *J*(H–P) 8.1, PMe], 1.52 (18 H, s, C_6Me_6), 7.02—7.14 (3 H, m, $H_m + H_p$), 7.33 [2 H, ddd, $J(H_o\text{–}H_m)$ 9.2, $J(H_o\text{–}H_p)$ 1.8, *J*(H–P) 7.4, H_o]

[a] Found (calc.) (%). [b] Spectra determined at 200 MHz, with the exception of the spectrum of complex (**7**), run at 300 MHz; given as chemical shift (δ) [relative intensity, multiplicity, coupling (*J* in Hz), assignment]; $[^2H_6]$benzene. [c] Fischer projection corresponding to the enantiomer, which is shown in Figure 1.

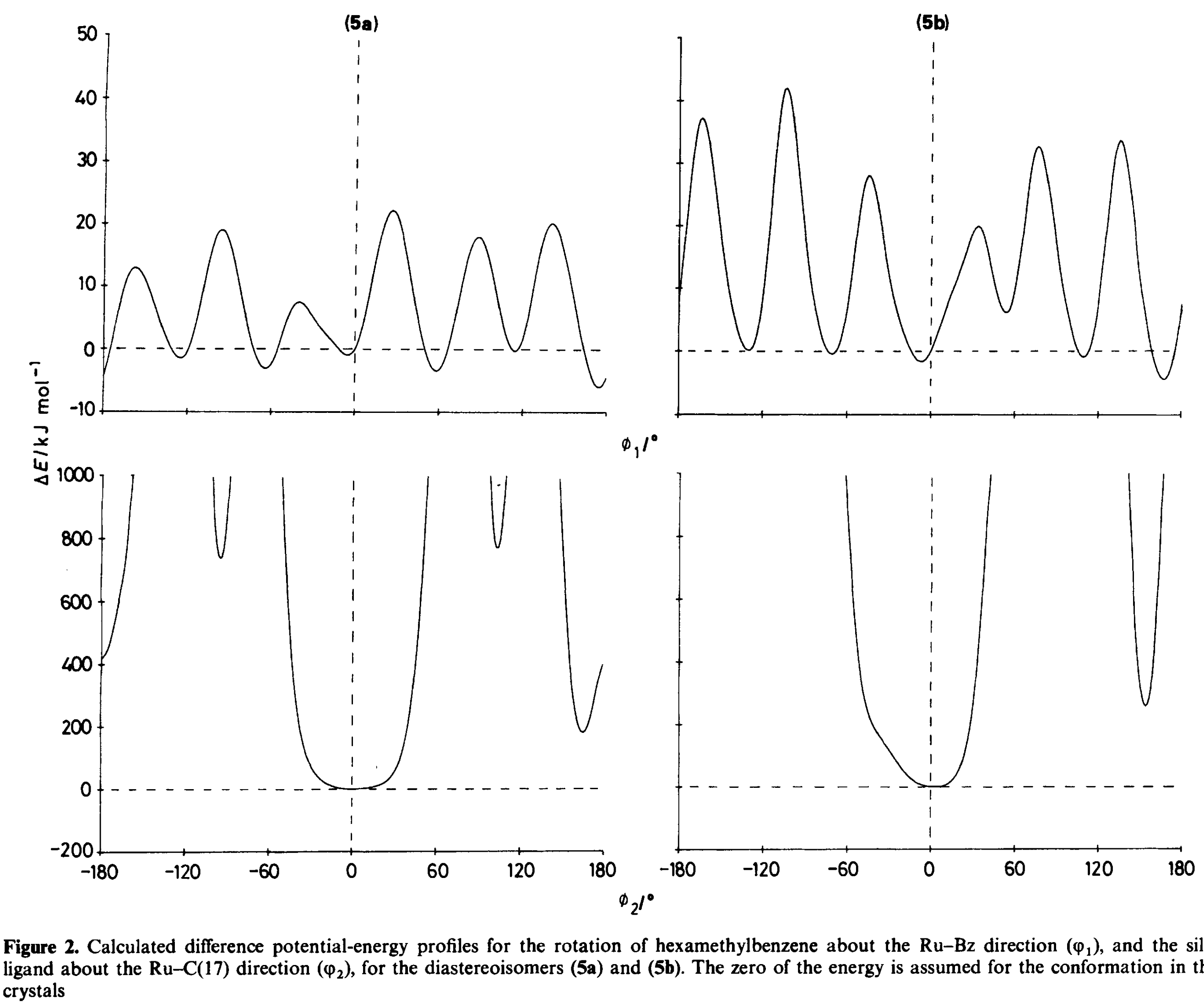

Figure 2. Calculated difference potential-energy profiles for the rotation of hexamethylbenzene about the Ru–Bz direction (φ_1), and the silyl ligand about the Ru–C(17) direction (φ_2), for the diastereoisomers (**5a**) and (**5b**). The zero of the energy is assumed for the conformation in the crystals

librations (see the ORTEP ellipsoids of Figures 1 and 4) and do not satisfy Hirshfeld's rigid-body postulate.[8] The relevant results of these analyses are compared in Table 4, which shows that the overall thermal motion in these compounds is quite similar to that found in the analogous iridium derivative $[\overline{Ir(C_6H_4}PPh_2)(CH_2SiMe_3)(\eta^5\text{-}C_5Me_5)]$.[3c] In the following discussion all the conventions applied in that paper for averaging and comparing data are followed.

Description of the structures of compounds (**4**), (**5a**), (**5b**), *and* (**6**). The molecular structures of these complexes are quite similar to that of the analogous iridium derivative.[3c] In particular, neither the substitution of the bulky C_5Me_5 by the bulkier C_6Me_6 ligand nor the substitution of the phenyl by the methyl groups in the phosphine changes the main geometrical features of these molecules. Nevertheless, small but significant differences are observed in the C_nMe_n centroid–metal distance, which is significantly longer in the case of the iridium derivative [Ir–Cp 1.892(7) Å; Cp = centroid of C_5Me_5] than in the ruthenium complexes (**4**)—(**6**) [Ru–Bz 1.762(3) Å (av.); Bz = centroid of C_6Me_6]. Moreover, comparing the metal–phosphorus distances [Ir–P 2.257(2), Ru–P 2.299(4) Å (av.), $\Delta/\sigma = 9.4$], the rule pointed out previously[3c] that in these 'three-legged piano-stool' complexes the longer is the C_nMe_n–M distance the shorter is the P(phosphine)–M bond is confirmed. This supports the idea that the approach of the phosphine ligand (and in general the ligands at the 'legs') to the metal is conditioned by the room left by the approach of the C_nMe_n ligand and *vice versa.* The angles in the co-ordination polyhedron show the same trends as those observed in the iridium derivative.[3c]

It should be noted that the metal is asymmetrically surrounded by four different ligands, so it is a chiral centre. In the crystals of the four compounds both enantiomers are present, the space group being centrosymmetrical. As already observed, the amount of diastereoisomer (**5a**) formed is twice that of diastereoisomer (**5b**). It is possible that this diastereoselectivity is justified by steric effects, as indicated by the results of van der Waals potential-energy calculations shown in Figure 2. In this figure the curves show the variation of the difference in potential energy ($\Delta E = E - E_o$, where E_o is the energy for the

Table 2. Fractional co-ordinates (× 10^4) for compounds (**4**), (**5a**), (**5b**), (**6**), and (**7**)

Atom	*X*/*a*	*Y*/*b*	*Z*/*c*
Compound (**4**)			
Ru	2 455.4(10)	1 280.3(6)	2 582.9(5)
P	4 474(3)	987(2)	2 383(2)
Si	1 251(4)	1 664(2)	656(2)
C(1)	706(12)	1 961(9)	2 826(7)
C(2)	1 893(13)	2 381(8)	3 206(7)
C(3)	2 897(12)	1 930(8)	3 672(6)
C(4)	2 736(11)	1 051(7)	3 796(6)
C(5)	1 605(13)	631(9)	3 429(7)
C(6)	595(11)	1 103(10)	2 961(7)
C(1M)	−399(12)	2 459(10)	2 363(7)
C(2M)	1 977(13)	3 337(9)	3 097(7)
C(3M)	4 064(13)	2 380(10)	4 091(7)
C(4M)	3 798(14)	611(9)	4 336(7)
C(5M)	1 448(15)	−295(9)	3 563(7)
C(6M)	−705(13)	676(10)	2 589(8)
C(11)	3 764(11)	65(8)	1 895(6)
C(12)	4 130(12)	−620(8)	1 540(7)
C(13)	3 217(14)	−1 221(9)	1 258(6)
C(14)	1 986(13)	−1 140(8)	1 368(6)
C(15)	1 591(12)	−441(8)	1 721(6)
C(16)	2 484(12)	190(7)	1 988(6)
C(17)	2 142(11)	2 001(8)	1 583(6)
C(19)	−338(12)	1 181(10)	656(7)
C(20)	2 206(12)	942(8)	200(6)
C(21)	882(13)	2 659(9)	73(7)
C(71)	5 856(11)	643(8)	3 100(6)
C(72)	6 664(11)	1 231(9)	3 507(7)
C(73)	7 699(13)	967(10)	4 067(8)
C(74)	7 952(14)	141(11)	4 225(8)
C(75)	7 154(14)	−453(9)	3 817(8)
C(76)	6 117(12)	−195(9)	3 252(7)
C(81)	5 283(10)	1 621(8)	1 830(6)
C(82)	5 714(11)	1 303(9)	1 264(7)
C(83)	6 333(14)	1 797(11)	842(7)
C(84)	6 508(13)	2 635(13)	989(9)
C(85)	6 136(14)	2 972(9)	1 549(10)
C(86)	5 490(13)	2 463(10)	1 966(8)
Compound (**5a**)			
Ru	−2 066.0(3)	−460.3(2)	−2 848.0(3)
P	−2 508.0(10)	532.7(7)	−1 857.6(9)
Si	−2 076.1(12)	−1 661.6(9)	−604.4(11)
C(1)	−1 066(5)	−1 288(3)	−3 637(4)
C(2)	−464(4)	−604(4)	−3 476(4)
C(3)	−981(5)	71(3)	−3 866(4)
C(4)	−2 079(4)	50(3)	−4 451(4)
C(5)	−2 659(4)	−616(3)	−4 565(4)
C(6)	−2 154(5)	−1 289(3)	−4 155(4)
C(1M)	−491(7)	−2 015(4)	−3 275(6)
C(2M)	732(5)	−598(6)	−2 860(6)
C(3M)	−309(7)	792(4)	−3 717(6)
C(4M)	−2 614(7)	750(4)	−4 953(5)
C(5M)	−3 823(5)	−655(4)	−5 214(5)
C(6M)	−2 810(6)	−2 024(3)	−4 338(5)
C(11)	−3 846(4)	105(3)	−1 904(4)
C(12)	−4 810(5)	247(3)	−1 530(5)
C(13)	−5 674(4)	−257(4)	−1 763(5)
C(14)	−5 549(4)	−881(3)	−2 345(4)
C(15)	−4 573(4)	−1 026(3)	−2 718(4)
C(16)	−3 662(4)	−536(3)	−2 490(3)
C(17)	−1 401(4)	−987(3)	−1 362(4)
C(19)	−2 719(5)	−2 458(3)	−1 421(5)
C(20)	−3 159(5)	−1 255(4)	85(5)
C(21)	−982(5)	−2 077(4)	430(5)
C(71)	−2 746(4)	1 467(3)	−2 398(4)
C(72)	−1 899(4)	1 999(3)	−2 242(4)
C(73)	−2 054(5)	2 708(3)	−2 653(4)
C(74)	−3 061(5)	2 906(3)	−3 230(5)
C(75)	−3 908(5)	2 394(3)	−3 397(5)
C(76)	−3 741(4)	1 686(3)	−2 983(4)
C(81)	−1 901(5)	743(3)	−504(4)
Compound (**5b**)			
Ru	2 291.6(2)	1 515.9(2)	2 312.8(2)
P	2 792.8(8)	1 912.0(8)	4 410.5(8)
Si	2 875.4(10)	4 436.7(9)	1 436.4(11)
C(1)	1 236(3)	1 278(3)	385(3)
C(2)	466(3)	1 148(3)	1 345(3)
C(3)	765(3)	322(3)	2 273(3)
C(4)	1 824(3)	−391(3)	2 285(4)
C(5)	2 603(3)	−223(3)	1 373(4)
C(6)	2 287(3)	603(3)	400(3)
C(1M)	872(4)	2 129(4)	−635(4)
C(2M)	−674(4)	1 872(4)	1 296(5)
C(3M)	−62(5)	131(5)	3 253(5)
C(4M)	2 060(5)	−1 359(4)	3 218(5)
C(5M)	3 724(4)	−950(4)	1 377(6)
C(6M)	3 059(4)	668(5)	−655(4)
C(11)	4 229(3)	2 257(3)	4 031(3)
C(12)	5 292(4)	2 599(4)	4 667(4)
C(13)	6 253(4)	2 604(4)	3 992(5)
C(14)	6 141(4)	2 239(4)	2 754(5)
C(15)	5 068(3)	1 882(4)	2 128(4)
C(16)	4 060(3)	1 908(3)	2 757(3)
C(17)	1 988(3)	3 400(3)	2 204(3)
C(19)	3 607(5)	3 864(5)	46(5)
C(20)	4 043(5)	5 096(4)	2 588(5)
C(21)	1 859(5)	5 685(5)	834(6)
C(71)	3 074(4)	758(4)	5 560(4)
C(81)	2 095(4)	3 040(4)	5 344(3)
C(82)	2 727(5)	3 876(5)	6 073(5)
C(83)	2 146(6)	4 685(5)	6 810(5)
C(84)	956(6)	4 669(5)	6 818(5)
C(85)	304(5)	3 840(5)	6 084(7)
C(86)	884(4)	3 045(5)	5 361(5)

Table 2 (*continued*)

Atom	*X*/*a*	*Y*/*b*	*Z*/*c*
Compound (**6**) (molecule A)			
Ru	3 199.1(3)	4 656.2(3)	2 393.2(3)
P	3 480.0(9)	3 232.7(9)	3 186.9(11)
Si	719(1)	4 641(1)	2 530(1)
C(1)	3 034(4)	5 762(4)	1 088(4)
C(2)	3 580(4)	4 897(4)	632(4)
C(3)	4 404(4)	4 458(4)	1 208(5)
C(4)	4 670(4)	4 894(4)	2 242(5)
C(5)	4 096(4)	5 717(4)	2 714(4)
C(6)	3 274(4)	6 175(4)	2 133(5)
C(1M)	2 193(5)	6 281(5)	438(6)
C(2M)	3 276(5)	4 455(5)	−491(5)
C(3M)	5 011(5)	3 567(5)	678(7)
C(4M)	5 597(4)	4 502(6)	2 814(7)
C(5M)	4 380(6)	6 155(5)	3 842(5)
C(6M)	2 697(6)	7 102(4)	2 607(6)
C(11)	2 949(3)	3 833(3)	4 436(4)
C(12)	2 780(4)	3 620(4)	5 519(4)
C(13)	2 372(4)	4 351(5)	6 269(4)
C(14)	2 170(4)	5 267(4)	5 939(4)
C(15)	2 355(4)	5 481(4)	4 851(4)
C(16)	2 744(3)	4 760(3)	4 058(4)
C(17)	1 865(3)	4 331(4)	1 813(4)
C(19)	378(4)	5 946(4)	2 925(6)
C(20)	598(4)	3 978(4)	3 787(5)
C(21)	−216(4)	4 374(5)	1 504(5)
C(71)	4 651(4)	2 627(4)	3 609(5)
C(81)	2 968(4)	2 225(4)	2 733(5)
Compound (**6**) (molecule B)			
Ru	1 775.3(3)	398.7(3)	−2 664.1(3)
P	1 258(1)	1 369(1)	−1 101(1)
Si	4 026(1)	1 030(1)	−2 057(1)
C(1)	2 071(4)	−135(6)	−4 478(4)
C(2)	1 312(6)	675(4)	−4 447(5)
C(3)	525(4)	671(5)	−3 825(6)
C(4)	479(4)	−120(6)	−3 231(5)
C(5)	1 233(5)	−880(4)	−3 213(5)
C(6)	2 030(4)	−909(4)	−3 846(5)
C(1M)	2 901(7)	−174(9)	−5 234(7)
C(2M)	1 392(9)	1 523(7)	−5 121(7)
C(3M)	−329(6)	1 473(7)	−3 785(9)
C(4M)	−402(6)	−183(9)	−2 604(8)
C(5M)	1 234(9)	−1 767(6)	−2 591(7)
C(6M)	2 813(7)	−1 790(6)	−3 920(8)
C(11)	1 977(3)	495(4)	−288(4)
C(12)	2 174(4)	358(4)	844(4)
C(13)	2 778(4)	−474(5)	1 110(5)
C(14)	3 157(4)	−1 138(4)	261(5)
C(15)	2 954(4)	−984(4)	−857(5)
C(16)	2 358(3)	−155(3)	−1 168(4)
C(17)	2 851(4)	1 230(4)	−2 729(4)
C(19)	4 719(5)	−166(5)	−2 482(6)
C(20)	4 078(4)	1 199(4)	−486(5)
C(21)	4 668(4)	1 907(5)	−2 590(6)
C(71)	68(4)	1 557(5)	−572(5)
C(81)	1 516(5)	2 542(4)	−748(5)
Compound (**7**)			
Ru	1 438.8(3)	376.1(4)	696.5(2)
P	976.4(12)	−1 154.8(14)	202.1(9)
Si(1)	1 791(2)	326(3)	2 454(1)
Si(2)	3 803(2)	138(2)	1 007(2)
C(1)	226(4)	1 358(5)	151(4)
C(2)	673(5)	1 771(5)	791(4)
C(3)	1 596(6)	2 026(6)	966(4)
C(4)	2 060(6)	1 813(7)	534(5)
C(5)	1 631(6)	1 404(7)	−88(4)
C(6)	741(5)	1 117(6)	−266(3)
C(7)	1 285(6)	−226(7)	1 607(4)
C(8A)	2 985(21)	1 015(26)	2 636(17)
C(9A)	1 316(25)	1 737(26)	2 562(16)
C(10A)	1 444(43)	−322(40)	3 050(28)
C(8B)	1 696(31)	1 513(40)	2 642(24)
C(9B)	1 310(26)	−758(28)	3 005(17)
C(10B)	2 973(32)	−232(34)	2 870(24)
C(8C)	1 807(22)	−565(28)	3 125(16)
C(9C)	2 979(18)	521(24)	2 771(14)
C(10C)	1 100(21)	1 387(27)	2 566(16)
C(11)	2 743(5)	−347(6)	1 054(4)
C(12)	4 668(7)	−885(9)	1 349(8)
C(13)	4 256(7)	1 328(9)	1 488(8)
C(14)	3 749(8)	358(9)	111(8)
C(15)	1 274(5)	−2 335(6)	679(4)
C(16)	1 352(6)	−1 400(8)	−502(4)

conformation found in the crystal) calculated after rotation of the hexamethylbenzene ring around the Ru–Bz direction (φ_1) or of the silyl ligand around the Ru–C(17) bond (φ_2). From these data it appears that the energy barriers for these rotations are significantly higher for the diastereoisomer (**5b**) that is formed in smaller amount.

The plane of the C_6Me_6 ligand is perpendicular to the Ru–Bz vector, as found with C_5Me_5 in respect of the Ir–Cp vector.[3c] Its orientation seems conditioned by the tendency of the Ru–P bond to be staggered with respect to the Bz–C(3) and Bz–C(4) directions, as shown by the Newman projection of Figure 3(*a*). No regular trends seem to be present in the distances between Ru and the carbon atoms of the ring, while a small but significant alternating lengthening and shortening [av. Δ = 0.026(3) Å] of the C–C bonds in the ring is observed in all complexes, as shown by the averaged data of Table 3. This kind of deformation that makes the symmetry of the benzene ring C_{3v}, rather than D_{6h} as for the free molecule, has been observed in other cases of η-co-ordinated benzene, like (benzene)tricarbonylchromium[9] where the *cis* bonds (*i.e.* those intersecting the projections of the metal–other ligand bonds) are lengthened to 1.423 Å [in our compounds 1.430(3) Å (av.)] and the *trans* bonds (*i.e.* those that do not intersect the projections of the metal–other ligand bonds) are shortened to 1.406 Å [in our compounds 1.404(3) Å (av.)]. As shown by the Newman projection of Figure 3(*a*) the orientation of the benzene ring with respect to the other ligand atoms is as shown below and

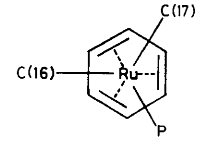

its bonding to the metal is quite similar to that found in $[Cr(C_6H_6)(CO)_3]$.[9]

Small displacements from planarity are observed for the C_6Me_6 ring, that are not significant except in the case of (**4**), as shown by the following parameters (Δ is the displacements of the ring atoms from the least-squares mean plane and Q is the Cremer and Pople total puckering amplitude[10]).

The analysis in terms of displacement asymmetry parameters[11] shows that the deformations in (**5a**), (**5b**), and in the two molecules of (**6**) are of the same twist type with two local approximate two-fold axes mutually perpendicular, one

Table 3. Comparison of bond distances (Å) and angles (°) for complexes (**4**), (**5a**), (**5b**) and (**6**) with estimated standard deviations (e.s.d.s) in parentheses

				(**6**)		
	(**4**)	(**5a**)	(**5b**)	molecule A	molecule B	Average
(*a*) Co-ordination sphere						
Ru–P	2.310(4)	2.316(2)	2.295(1)	2.288(2)	2.301(1)	2.299(4)
Ru–C(C_6Me_6) (av.)	2.271(5)	2.258(6)	2.270(7)	2.261(7)	2.253(6)	2.263(4)
Ru–Bz	1.771(14)	1.766(6)	1.762(4)	1.761(6)	1.759(6)	1.762(3)
Ru–C(16)	2.068(12)	2.086(5)	2.091(4)	2.098(5)	2.095(5)	2.091(3)
Ru–C(17)	2.172(12)	2.179(5)	2.178(4)	2.188(5)	2.184(6)	2.181(2)
Bz–Ru–P	139.2(4)	138.7(2)	138.7(1)	137.1(2)	137.3(2)	138.3(3)
Bz–Ru–C(16)	131.6(6)	131.4(2)	134.8(2)	132.5(2)	131.8(3)	132.7(3)
Bz–Ru–C(17)	124.8(5)	124.9(2)	125.4(2)	124.8(2)	125.1(3)	125.0(1)
P–Ru–C(16)	67.0(4)	66.9(1)	66.6(1)	67.0(1)	67.3(1)	66.9(1)
P–Ru–C(17)	85.4(3)	85.7(1)	84.4(1)	86.3(2)	85.3(2)	85.2(3)
C(16)–Ru–C(17)	89.0(4)	89.5(2)	85.3(1)	89.7(2)	90.6(2)	87.3(11)
[Ru–Bz] $\wedge$ [C(1)—C(6)]	89.5(4)	89.9(2)	89.0(1)	89.2(2)	89.5(2)	89.2(2)
(*b*) C_6Me_6 ligand						
C–C *cis** (av.)	1.439(10)	1.421(4)	1.440(3)	1.426(4)	1.415(12)	1.430(3)
C–C *trans** (av.)	1.404(10)	1.393(11)	1.409(4)	1.413(6)	1.394(8)	1.404(3)
C–CH_3 (av.) 1.518(3) [min. 1.488(17), max. 1.549(18)]						
C–C–C endocyclic (av.) 120.0(1) [min. 117.2(12), max. 122.6(13)]						
CH_3 ··· [C(1)—C(6)] (av.)	0.077(13)	0.058(24)	0.068(26)	0.053(34)	0.064(28)	0.070(9)
CH_3 $\wedge$ [C(1)—C(6)] (av.)	3.0(4)	2.2(8)	2.6(9)	2.3(10)	2.7(7)	2.7(2)
C_6Me_6 effective cone angle	157	158	159	160	158	158.4(5)
(*c*) Silyl ligand						
Si–CH_2	1.866(11)	1.844(5)	1.861(4)	1.856(5)	1.852(5)	1.855(3)
Si–CH_3 (av.)	1.879(18)	1.873(4)	1.884(5)	1.883(7)	1.872(7)	1.879(3)
CH_2–Si–CH_3 min.	107.3(6)	108.3(3)	107.8(2)	108.5(3)	107.8(3)	108.0(2)
max.	113.6(6)	114.9(3)	117.3(2)	116.6(3)	117.1(3)	116.5(5)
CH_3–Si–CH_3 min.	106.1(6)	106.4(3)	105.5(3)	105.0(3)	105.4(3)	105.6(3)
max.	109.9(6)	108.0(3)	107.4(3)	108.9(3)	108.2(3)	108.2(3)
(*d*) Metallaphosphacyclobutane ring						
P–C(11)	1.798(12)	1.797(5)	1.800(4)	1.783(5)	1.792(5)	1.794(3)
C(11)–C(16)	1.426(18)	1.419(7)	1.406(5)	1.419(7)	1.405(6)	1.411(3)
Ru ··· C(11)	2.863(13)	2.863(5)	2.858(4)	2.855(5)	2.840(5)	2.855(4)
P ··· C(16)	2.424(12)	2.435(5)	2.415(4)	2.426(4)	2.443(5)	2.428(5)
Ru–P–C(11)	87.4(4)	87.3(8)	87.7(1)	88.1(2)	87.0(2)	87.6(2)
P–C(11)–C(16)	96.8(8)	97.8(3)	97.0(2)	97.9(3)	98.9(4)	97.6(3)
Ru–C(16)–C(11)	108.7(8)	108.0(3)	108.0(2)	107.0(3)	106.8(3)	107.6(3)
Ru ··· [C(11)—C(16)]	0.071(2)	0.027(1)	0.034(1)	0.063(1)	0.085(1)	0.053(11)
P ··· [C(11)—C(16)]	0.104(4)	0.016(2)	−0.232(1)	0.090(2)	0.060(2)	0.154(44)
(*e*) Orthometallated benzene						
C(11)–C(12)	1.381(18)	1.374(8)	1.390(5)	1.391(7)	1.393(7)	1.388(3)
C(12)–C(13)	1.374(18)	1.382(8)	1.384(7)	1.382(7)	1.389(9)	1.383(4)
C(13)–C(14)	1.378(21)	1.374(9)	1.373(9)	1.383(9)	1.390(8)	1.380(4)
C(14)–C(15)	1.408(19)	1.388(8)	1.402(6)	1.403(8)	1.382(8)	1.396(4)
C(15)–C(16)	1.390(17)	1.408(6)	1.399(5)	1.398(6)	1.396(8)	1.400(3)
C(12)–C(11)–C(16)	123.8(11)	124.5(5)	124.9(4)	123.9(4)	123.8(5)	124.3(2)
C(11)–C(12)–C(13)	118.7(12)	118.0(5)	117.4(4)	118.2(5)	117.6(5)	117.8(2)
C(12)–C(13)–C(14)	119.0(12)	120.0(5)	119.9(4)	119.7(5)	120.0(6)	119.2(2)
C(13)–C(14)–C(15)	123.1(13)	122.0(5)	122.0(4)	121.9(5)	121.2(6)	121.9(2)
C(14)–C(15)–C(16)	119.0(12)	120.4(5)	120.2(5)	120.2(5)	121.0(5)	120.4(2)
C(15)–C(16)–C(11)	116.4(11)	115.1(4)	115.5(3)	116.0(4)	116.3(5)	115.7(2)
Ru–C(16)–C(15)	134.7(10)	136.8(4)	136.5(3)	137.0(4)	136.8(4)	136.7(2)
P–C(11)–C(12)	139.3(10)	137.7(4)	137.6(3)	138.1(4)	137.2(4)	137.7(2)

(*f*) Phosphine ligand

P–C(Ph) (av.)	1.823(3)	Ru–P–C(Ph)(av.)	123.7(9)
P–C(Me) (av.)	1.830(2)	Ru–P–C(Me) (av.)	122.8(22)
P–C–C (av.)	120.9(6)		

* See text.

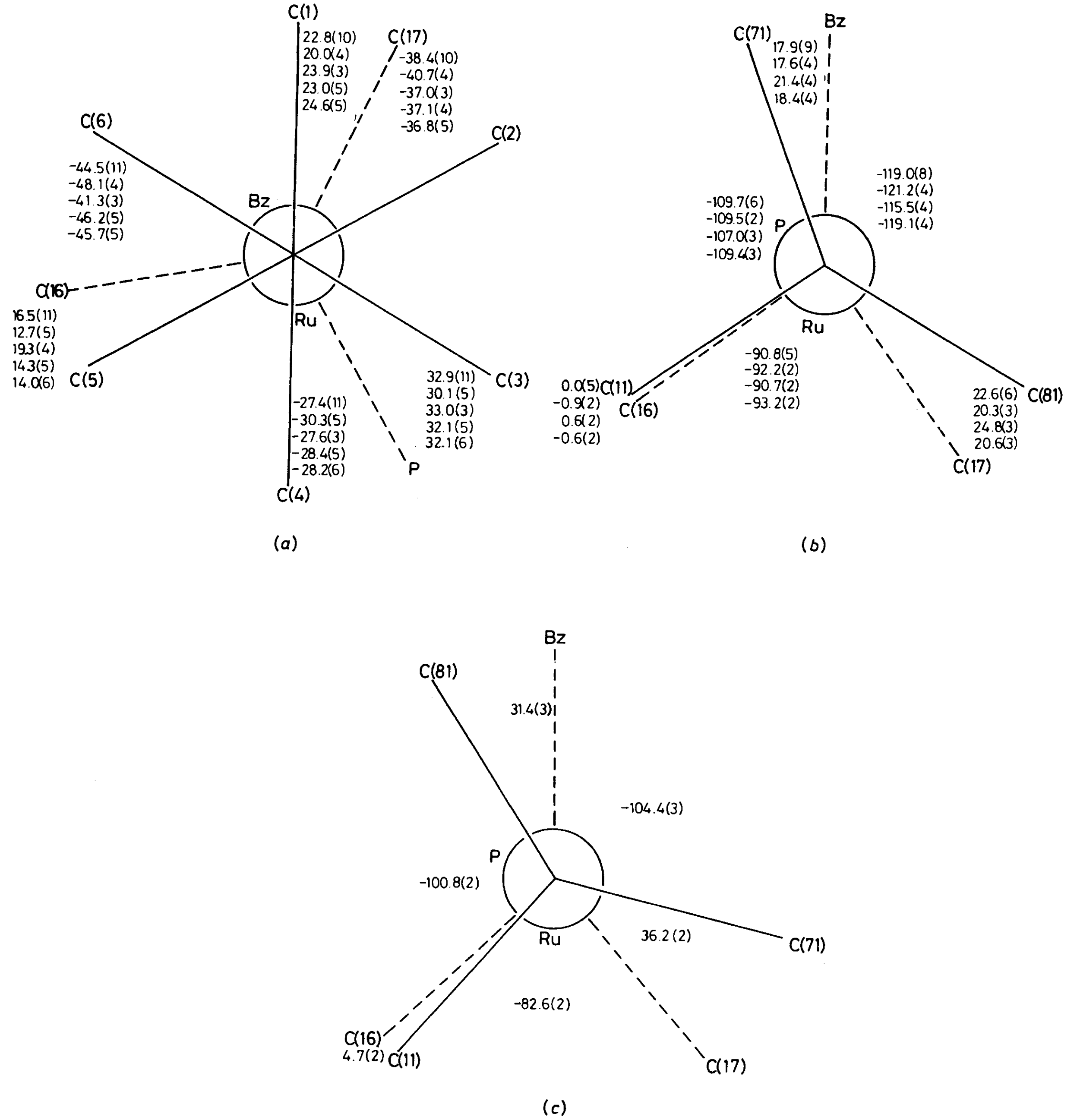

Figure 3. Newman projections: (*a*) along Bz–Ru, showing the orientation of the η-C_6Me_6 ligand; (*b*) and (*c*) along P–Ru in complexes (**4**), (**5a**), (**6**) molecules A and B, and (**5b**), respectively. Each quintuplet or quartet of angle values (°) refers to the complexes in the same order from the top to the bottom. In (*a*) the C(1)–C(2), C(3)–C(4), C(5)–C(6) bond distances are lengthened with respect to C(2)–C(3), C(4)–C(5), C(6)–C(1) which are shortened (see text)

Compound	$\Sigma(\Delta/\sigma)^2$	Q/Å
(**4**)	3.6	0.023(12)
(**5a**)	61.3	0.042(5)
(**5b**)	69.7	0.032(4)
(**6**) molecule A	51.6	0.041(6)
(**6**) molecule B	35.4	0.038(6)

running along two opposite vertices, the other along two opposite sides of the hexagon. As observed for the η^5-C_5Me_5 metal derivatives, the methyl groups are displaced from the plane of the ring, all in opposite directions with respect to the metal [except C(2M) for (**5a**) and (**6**) (both molecules), and C(5M) for (**5b**) and (**6**) (molecule A)], but these displacements are smaller [av. 0.07(1) Å] than those found in the η^5-C_5Me_5 iridium derivative [av. 0.14(2) Å].[3c]

As found for similar orthometallated phenylphosphine complexes, the orthometallated benzene ring becomes deformed mainly in the endocyclic angles at C(11), C(12), and C(16). The first angle, involving the carbon atom bound to phosphorus, widens to 124.3(2)° (av.), while the other two become narrower, particularly that involving the carbon atom C(16) bound to the metal [115.7(2)° (av.)].

The metallaphosphacyclobutane ring is planar and essentially coplanar with the phenyl ring, the largest deviation from coplanarity being only 7.7(1)° in (**5b**). The planarity of the metallacycle is imposed by the tendency of the phosphorus

Table 4. Results of the anisotropic atomic displacement analysis *

		Group libration amplitudes/°					
		(4)	**(5a)**	**(5b)**	(6)		(7)
Librating group	Libration along				molecule A	molecule B	
C(1)—C(6)	Ru–Bz	4.6(10)	7.6(6)	4.4(6)	6.8(5)	10.2(4)	4.0(7)
C(1M)—C(6M)	Ru–Bz	4.9(3)	7.6(2)	4.0(3)	5.5(2)	9.6(2)	—
C(12)—C(16)	P–C(11)	1.5(33)	3.1(13)	—	0.8(34)	4.1(11)	—
C(12)—C(16)	Bz1–NP1	—	—	3.6(9)	—	—	—
C(72)—C(76)	P–C(71)	2.0(48)	0.6(14)	—	—	—	—
C(81)—C(86)	P–C(81)	2.1(45)	—	—	—	—	—
C(81)—C(86)	Bz8–NP8	—	—	3.9(10)	—	—	—
C(19), C(20), C(21)	Si–C(17)	5.5(9)	7.2(7)	2.6(6)	5.1(6)	4.9(8)	—
C(71)	Ru–P	—	—	4.0(18)	2.0(34)	2.6(33)	—
C(81)	P–C(71)	—	6.4(12)	—	—	—	—
C(81)	Ru–P	—	—	—	2.6(29)	5.2(17)	—
Si(2), C(12), C(13), C(14)	Ru–C(11)	—	—	—	—	—	3.8(17)

			Rigid body		Internal motions	
Compound	$\bar{\Delta}$	$\bar{\sigma}(U_o)$	$w\Delta U$	R_{wU}	$w\Delta U$	R_{wU}
(4)	0.014(18)	0.0088	0.004 4(46)	0.184	0.003 3(38)	0.136
(5a)	0.014(24)	0.0038	0.004 3(45)	0.167	0.002 2(26)	0.084
(5b)	0.008(11)	0.0025	0.001 9(20)	0.109	0.001 4(17)	0.080
(6) molecule A	0.009(12)	0.0035	0.002 8(30)	0.119	0.001 5(20)	0.064
(6) molecule B	0.016(25)	0.0049	0.004 4(47)	0.175	0.001 7(21)	0.065
(7)	0.012(16)	0.0052	0.004 0(45)	0.124	0.002 4(30)	0.077

* Bz = Centroid of the C(1)—C(6) ring, Bz1 = centroid of the C(12)—C(16) ring, Bz8 = centroid of the C(81)—C(86) ring, NP1 = normal to the C(12)—C(16) plane through Bz1, NP8 = normal to the [C(81)—C(86)] plane through Bz8; $\bar{\Delta}$ = mean difference of the mean-square vibrational amplitudes along the interatomic directions for all pairs of atoms, $\Delta U = U_{ij}(\text{obs.}) - U_{ij}(\text{calc.})$, $\bar{\sigma}(U_o)$ = mean e.s.d. of U_o values, $w\Delta U = [\Sigma(w\Delta U)^2/\Sigma w^2]^{\frac{1}{2}}$, and $R_{wU} = [\Sigma(w\Delta U)^2/\Sigma(wU_o)^2]^{\frac{1}{2}}$.

Table 5. Selected bond distances (Å) and angles (°) for complex (7), with e.s.d.s in parentheses

(*a*) Co-ordination sphere

Ru–P	2.276(2)	Ru–C(7)	2.177(9)
Ru–C(Ph) (av.)	2.243(15)	Ru–C(11)	2.178(8)
Ru–Bz	1.744(8)		
Ru–P–C(15)	121.0(3)	P–Ru–C(7)	88.2(2)
Ru–P–C(16)	112.9(3)	P–Ru–C(11)	84.0(2)
Ru–C(11)–Si(2)	128.0(4)	C(7)–Ru–C(11)	85.1(3)
Bz–Ru–P	127.9(3)	Ru–C(7)–Si(1)	125.1(5)
Bz–Ru–C(7)	128.0(4)	[Ru–Bz] ∧ [C(1)—C(6)]	90.0(5)
Bz–Ru–C(11)	128.7(4)		

(*b*) Phosphine ligand

P–C(1)	1.827(7)	P–C(16)	1.818(11)
P–C(15)	1.826(8)	C–C (phenyl) (av.)	1.406(9)
C(1)–P–C(15)	98.1(4)	C(15)–P–C(16)	102.0(4)
C(1)–P–C(16)	103.4(4)	C–C–C (phenyl) (av.)	119.8(6)

(*c*) Silyl ligand (not disordered)

Si(1)–C(7)	1.849(8)	Si(2)–C(11)	1.843(10)
Si(2)–C(12)	1.888(12)	Si(2)–C(13)	1.874(12)
Si(2)–C(14)	1.896(18)		

C–Si(2)–C (min., max.) 105.7(6), 116.9(5)

and ruthenium atoms to lie in the C(11)—C(16) benzene plane (see Table 3), probably as a consequence of conjugative effects, thus causing eclipsing of the Ru–C(16) and P–C(11) bonds, as shown in the Newman projections of Figure 3(*b*) and (*c*).

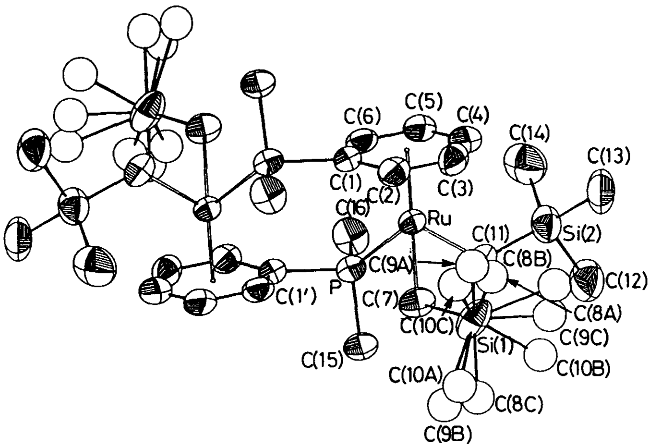

Figure 4. ORTEP drawing of complex (7) showing the cyclic structure of the molecule and the disorder involving the Si(1) silyl group. Thermal ellipsoids are at 40% probability

Description of the structure of complex (7). As shown by the ORTEP drawing of Figure 4, (7) consists of cyclic dimeric binuclear complex molecules with crystallographically imposed C_i symmetry, where the phosphine ligand is bridging two ruthenium atoms, one σ bonded by the phosphorus atom, the other η^6 bonded by the phenyl group.* The ring Ru–C(1)–P′–Ru′–C(1)′–P is puckered (Q = 0.701 Å) with a chair conformation. The co-ordination about the metal is of the 'three-legged piano-stool' type as in compounds (4)—(6), with the

---

* A similar binuclear complex $[\{Mo(\mu\text{-}\sigma,\eta^6\text{-}PPh_3)(PPh_3)[CN(CH_2)_3Me]\}_2]$ has been described.[12]

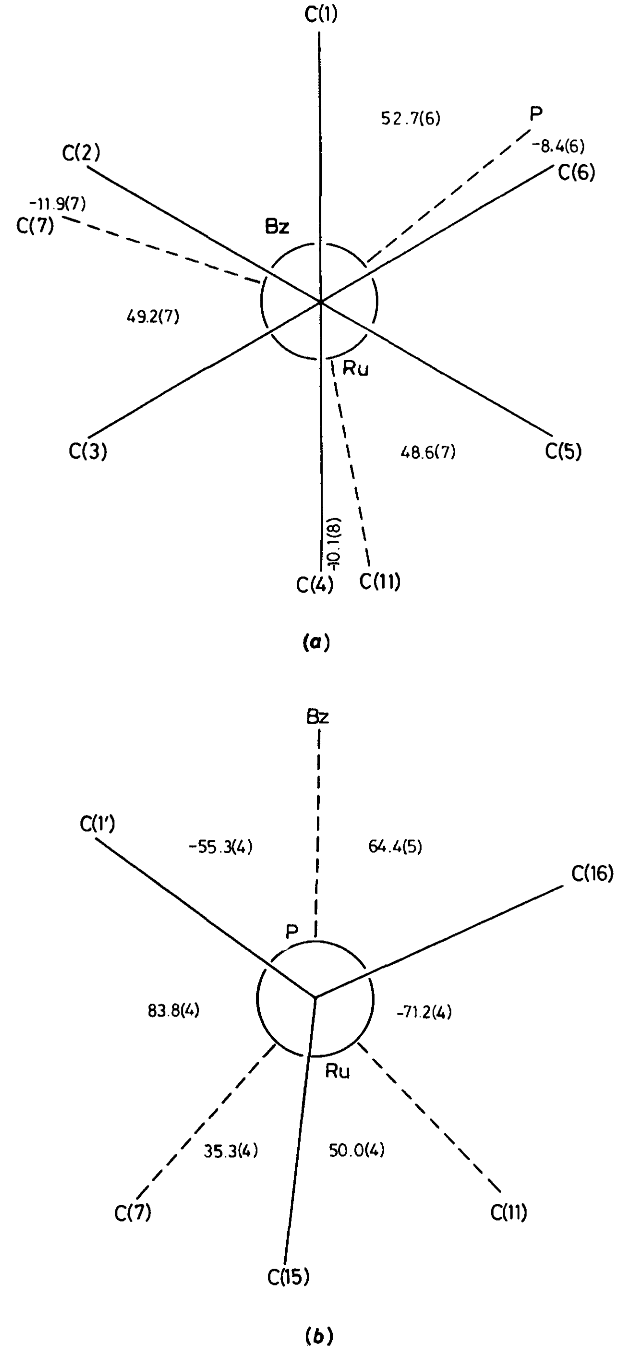

Figure 5. Newman projections about (*a*) Bz–Ru and (*b*) P–Ru for complex (7)

direction Ru–Bz perpendicular to the ring plane, but the orientation of the phenyl ring with respect to the other ligand atoms is nearly eclipsed with C(2), C(4), and C(6) shifted only 10° from overlapping the atoms C(7), C(11), and P respectively [Figure 5(*a*)]. On the contrary, eclipsing is now avoided by the bonds formed by P with respect to those formed by Ru [Figure 5(*b*)].

Relevant distances and angles concerning the molecule of (7) are collected in Table 5 which shows that these parameters do not differ greatly from the corresponding ones in (4)—(6), except for the angles about Ru which are more regular owing to the absence of constraints imposed by the orthometallation. Contrary to (4)—(6), no regular trends are observed for the endocyclic angles of the phenyl ring.

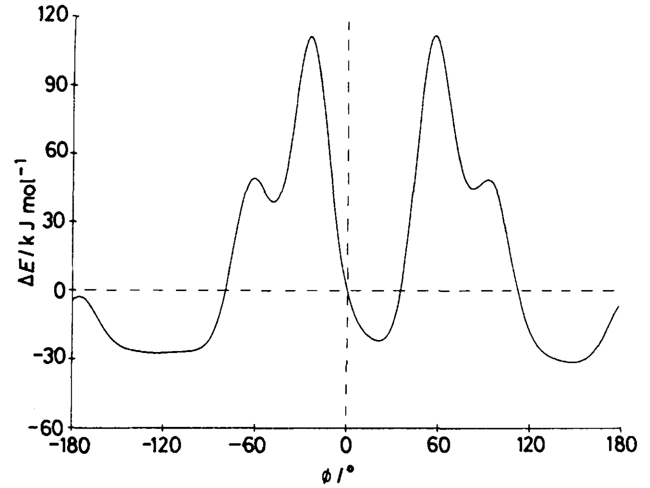

Figure 6. Calculated potential-energy profile for rotation of the Si(1) silyl group about the C(7)–Si(1) bond in complex (7). The starting conformation, φ = 0°, corresponds to the silyl group *trans* with respect to the C(7)–Ru bond. The three minima at φ = 20°, 147.5°, and φ = −125°, correspond to the three disordered orientations assumed with equal population by the silyl group

Conclusion

The reaction of the dichloro compounds (**1**)—(**3**) with the bulky $Mg(CH_2SiMe_3)Cl$ Grignard reagent gives directly and under mild conditions the orthometallated alkyl derivatives (**4**)—(**6**). We have recently reported[3] that a similar reaction between the isoelectronic system $[MCl_2(\eta^5\text{-}C_5Me_5)(PPh_3)]$ (M = Rh or Ir) and $Mg(CH_2SiMe_3)Cl$ or $Li(CH_2SiMe_3)$ leads to the corresponding bis(trimethylsilylmethyl) derivatives or to the orthometallated trimethylsilylmethyl compounds, depending on the experimental conditions. The absence of the dialkyl compounds in the case of ruthenium can be attributed to the more severe steric restrictions dictated by the C_6Me_6 ligand (effective C_6Me_6–Ru cone angle 157—160°, see Table 2), which are substantially higher than that of the C_5Me_5 ligand (C_5Me_5–Ru, cone angle 142; C_5Me_5–Ir, 146°).[3b,c] So, even by using $PMePh_2$ and PMe_2Ph, which are less sterically demanding than triphenylphosphine, there is not enough room left around the metal atom for two bulky alkyl groups to be accommodated. The dialkyl compound is sufficiently stable to be isolated only when the C_6Me_6 ligand is substituted by the less bulky phenyl group of the phosphine, as in the case of (**7**).

As for the mechanism by which the orthometallated compounds (**4**)—(**6**) are formed, we are confident that the chloroalkyl derivative (**8**) has a crucial role, as its conversion into (**6**) by further reaction with $Mg(CH_2SiMe_3)Cl$ seems to indicate, and we are studying this point in more detail.

Experimental

The reactions and manipulations of organometallics were carried out under dinitrogen or argon, using standard techniques. Solvents were dried and distilled prior to use. The compounds $[\{RuCl_2(\eta^6\text{-}C_6Me_6)\}_2]$,[13] $[RuCl_2(\eta^6\text{-}C_6Me_6)L]$ [L = PPh_3, (**1**); $PMePh_2$, (**2**); or PMe_2Ph, (**3**)],[14,15] $Mg(CH_2SiMe_3)Cl$,[16] $Mg(CH_2CMe_3)Cl$,[17] $Li(CH_2SiMe_3)$,[18] and $Li(CH_2CMe_3)$[19] were prepared as described. Nuclear magnetic resonance spectra were recorded on Varian Gemini 200 and VXR 300 instruments. Microanalyses were performed by the Laboratorio di Microanalisi of the Istituto di Chimica Organica, Facoltà di Farmacia, Università di Pisa.

(o-*Diphenylphosphinophenyl*-C[1], P)(η[6]-*hexamethylbenzene*)-

Table 6. Experimental data for the crystallographic analyses[a]

Compound	**(4)**	**(5a)**	**(5b)**	**(6)**	**(7)**
Formula	$C_{34}H_{43}PRuSi$	$C_{29}H_{41}PRuSi$	$C_{29}H_{41}PRuSi$	$C_{24}H_{39}PRuSi$	$C_{16}H_{33}PRuSi_2$
M	611.84	549.77	549.77	487.70	413.65
Space group	$P2_1/c$	$P2_1/a$	$P\bar{1}$	$P\bar{1}$	$C2/c$
a/Å	10.622(3)	12.215(8)	11.457(6)	14.633(4)	15.966(2)
b/Å	15.851(10)	17.920(10)	11.452(5)	14.527(4)	13.165(1)
c/Å	18.963(18)	13.023(7)	10.736(5)	11.936(3)	21.213(5)
α/°	—	—	91.96(1)	94.03(1)	—
β/°	103.64(2)	100.02(2)	96.39(1)	91.54(1)	109.94(1)
γ/°	—	—	87.92(1)	77.78(1)	—
U/Å^3	3 103(4)	2 807(3)	1 398(1)	2 473(1)	4 192(1)
Z	4	4	2	4	8
D_c/Mg m^{-3}	1.310	1.301	1.306	1.310	1.311
Diffractometer	Philips PW1100	Philips PW1100	Philips PW1100	Philips PW1100	Siemens AED
Reflections for lattice parameters:					
number	25	22	30	31	30
θ range/°	10.0—16.0	20.7—25.3	22.8—28.3	20.3—23.6	20.0—37.2
F(000)	1 280	1 152	576	1 024	1 728
Crystal size/mm	0.11 × 0.24 × 0.37	0.42 × 0.58 × 0.61	0.23 × 0.35 × 0.80	0.34 × 0.45 × 0.48	0.18 × 0.33 × 0.48
μ/mm^{-1}	0.603	0.659	0.662	0.739	7.976
Absorption correction (min., max.)	0.9527, 1.1335	—	—	—	0.756, 1.244
Extinction correction (min., max.)	0.8711, 1.0203	—	—	—	0.938, 1.162
Scan speed/° min	0.05	0.075	0.10	0.10	0.05—0.20
Scan width/°	1.60	1.60	1.80	1.40	1.2 + 0.14 tan θ
θ range/°	3—25	3—29	3—29	3—24	3—70
h range	−12 to 12	−16 to 16	−15 to 15	−16 to 16	−19 to 18
k range	0—18	0—24	−15 to 15	−16 to 16	0—16
l range	0—22	0—17	0—14	0—13	0—25
Standard reflection	0 2 5	$\bar{6}$ 0 1	$\bar{1}$ 2 4	3 1 6	5 6 2
No. of measured reflections	5 853	7 965	74 26	7 754	4 299
Condition for observed reflections	$I \geqslant 3\sigma(I)$	$I \geqslant 2\sigma(I)$	$I \geqslant 2\sigma(I)$	$I \geqslant 2\sigma(I)$	$I \geqslant 2\sigma(I)$
No. of reflections used in refinement	2 202	4 505	5 855	5 763	2 899
R(int)	0.0349	0.0302	—	—	0.0561
Max. least-squares shift to error ratio	0.46	0.69	0.44	0.54	0.2
Min., max. height in final Δρ/e Å^{-3}	−0.17, 0.14	−0.11, 0.14	−0.26, 0.60	−0.12, 0.21	−0.41, 0.28
No. of refined parameters	506	453	453	244	191
$R = \Sigma\lvert\Delta F\rvert/\Sigma\lvert F_o\rvert$	0.0599	0.0528	0.0435	0.0393	0.0593
$R' = [\Sigma w(\Delta F)^2/\Sigma wF_o^2]^{\frac{1}{2}}$	0.0550	0.0494	0.0600	0.0480	0.0867
$S = [\Sigma w(\Delta F)^2/(N - P)]^{\frac{1}{2}}$[b]	1.8338	1.6040	0.6432	1.0338	1.1192
k, g in $w = k/[\sigma^2(F_o) + gF_o^2]$	1.0	1.6741	0.7204, 0.003 68	1.0942, 0.000 65	1.000, 0.005

[a] Details in common: T = 293(2) K, Mo-K_α radiation (λ = 0.709 30 Å); no intensity variation; scan mode θ—2θ. [b] P = Number of parameters, N = number of observations.

[*trimethylsilylmethyl*)*ruthenium*(II) (**4**).—To a stirred suspension of complex (**1**) (0.189 g, 0.317 mmol) in pentane (30 cm^3) was added $Mg(CH_2SiMe_3)Cl$ (5.7 cm^3 of a 0.56 mol dm^{-3} solution in diethyl ether, 3.18 mmol) at room temperature over a period of 15 min. The reaction mixture was stirred for 24 h, then the orange-red solution was decanted and evaporated, and the residue extracted with pentane (60 cm^3). The pentane-soluble material was hydrolyzed at 0 °C with water (4 cm^3) and the organic layer dried over sodium sulphate. The pentane solution was concentrated to *ca.* 5 cm^3 and chromatographed through a column of neutral alumina. Elution with pentane–diethyl ether (10:1) gave a yellow band. Evaporation of the solvent gave an orange-yellow solid, complex (**4**) (0.048 g, 25%). The product was crystallized from pentane at −20 °C to give orange crystals.

(RR:SS)- *and* (RS:SR)-(η^6-*Hexamethylbenzene*)(o-*methylphenylphosphinophenyl*-C^{1}P)(*trimethylsilylmethyl*)*ruthenium*(II) (**5a**) *and* (**5b**).—To a stirred suspension of complex (**2**) (0.219 g, 0.41 mmol) in pentane (20 cm^3) was added $Mg(CH_2SiMe_3)Cl$ (7.5 cm^3 of a 0.55 mol dm^{-3} solution in ether, 4.1 mmol) at room temperature over a period of 30 min. The reaction mixture was stirred for 6 h, then the orange-yellow decanted solution was evaporated and the residue extracted with pentane (50 cm^3). The pentane extract was hydrolyzed with water (5 cm^3) at 0 °C and the organic layer dried over sodium sulphate. The pentane solution was concentrated to *ca.* 7 cm^3, and chromatographed through a column of neutral alumina. Elution with pentane gave a yellow band (A), and then 25% diethyl ether in pentane eluted an orange-yellow band (B). Band A was concentrated to *ca.* 4 cm^3 and rechromatographed: pentane eluted a band which on evaporation *in vacuo* gave an orange-yellow solid, complex (**5a**) (0.054 g, 24%). The product was crystallized from pentane to give yellow crystals. 30% Diethyl ether in pentane eluted a second yellow band which was combined with band B. Evaporation of band B gave a residue, which was dissolved in pentane (7 cm^3) and rechromatographed. Pentane eluted two yellow fractions: the first was evaporated *in vacuo* to give a solid which resulted a mixture of hexamethylbenzene and (**5a**); the second band gave, after evaporation, an orange-yellow solid (**5b**) (0.011 g, 4%). This product was crystallized from pentane at −20 °C to give orange crystals.

Reaction of Complex (**3**) *with* $Mg(CH_2SiMe_3)Cl$: *Formation of* (o-*Dimethylphosphinophenyl*-C^{1}P)(η^6-*hexamethylben-*

zene)(trimethylsilylmethyl)ruthenium(II) (**6**), Bis-(μ-*dimethylphosphinobenzene*-C^{1-6}:P)-bis[bis(*trimethylsilylmethyl*)-*ruthenium*(II)] (**7**), *and Chloro*(*dimethylphenylphosphine*)(η^6-*hexamethylbenzene*)(*trimethylsilylmethyl*)*ruthenium*(II) (**8**).—To a stirred suspension of complex (**3**) (0.425 g, 0.90 mmol) in pentane (50 cm^3) was added $Mg(CH_2SiMe_3)Cl$ (16.5 cm^3 of a 0.55 mol dm^{-3} solution in ether, 90 mmol) at room temperature over a period of 30 min. The reaction mixture was stirred for 8 h, then the orange-red solution was decanted and evaporated, and the residue was extracted with pentane (60 cm^3). The pentane extract was hydrolyzed at 0 °C with water (6 cm^3) and the organic layer dried over sodium sulphate. The pentane solution was concentrated to *ca.* 9 cm^3 and chromatographed through a column of neutral alumina. Elution with pentane gave a yellow band (A), 25% diethyl ether in pentane eluted a second orange-yellow band (B), and 50% diethyl ether in pentane eluted a third orange band (C). Band A was concentrated to *ca.* 5 cm^3 and rechromatographed: elution with pentane gave a yellow band which was concentrated and cooled to −20 °C to give orange-yellow crystals of complex (**7**) (0.075 g, 20%). Band B was evaporated to dryness, the residue dissolved in pentane (5 cm^3), and chromatographed again: elution with 20% diethyl ether in pentane gave an orange-yellow band which was evaporated to dryness. The residue was dissolved in pentane (5 cm^3) and cooled to −20 °C to give orange-yellow crystals of complex (**6**) (0.022 g, 5%). Band C was evaporated to dryness, the residue dissolved in pentane, and cooled to −20 °C to give orange-red crystals of complex (**8**) (0.052 g, 11%).

Reaction of Complex (**3**) *with* $Mg(CH_2SiMe_3)Cl$: *Formation of* (**8**).—Complex (**3**) (0.535 g, 1.14 mmol) was treated with $Mg(CH_2SiMe_3)Cl$ (2.7 cm^3 of a 0.63 mol dm^{-3} diethyl ether solution, 1.7 mmol) in diethyl ether (15 cm^3) for 18 h. Dioxane (0.3 cm^3) was added and the reaction mixture was stirred. The solvent was pumped off, the residue was added to pentane (40 cm^3) and hydrolyzed at 0 °C with water. The pentane solution was dried over Na_2SO_4, reduced in volume, and cooled to −20 °C to give orange-red crystals of complex (**8**) (0.359 g, 60%).

Reaction of Complex (**8**) *with* $Mg(CH_2SiMe_3)Cl$: *Formation of* (**6**) *and* (**7**).—Complex (**8**) (0.300 g, 0.58 mmol) was treated with $Mg(CH_2SiMe_3)Cl$ (1.38 cm^3 of a 0.63 mol dm^{-3} solution in diethyl ether, 0.87 mmol) in pentane (25 cm^3) for 3 h. The usual work-up followed by chromatographic purification gave crystals of complexes (**6**) (8%), (**7**) (35%), and (recovered) (**8**) (0.075 g).

Reaction of Complex (**8**) *with* LiMe: *Formation of* (*Dimethylphenylphosphine*)(η^6-*hexamethylbenzene*)*methyl*(*trimethylsilylmethyl*)*ruthenium*(II) (**9**).—To a stirred solution of complex (**8**) (0.200 g, 0.38 mmol) in pentane (15 cm^3) was added LiMe (2 cm^3 of a 2.16 mol dm^{-3} solution in Et_2O, 4.32 mmol) at room temperature. The reaction mixture was stirred for 30 h. The usual work-up, followed by chromatographic purification on neutral alumina (pentane as eluant), gave yellow crystals of complex (**9**) (0.101 g, 53%).

Crystal Structure Analysis of the Complexes (**4**)—(**7**).—Table 6 quotes the relevant data for the crystal structure analyses. The lattice parameters were refined by a least-squares procedure[20] using the Nelson and Riley extrapolation function.[21] All reflections were corrected for Lorentz and polarization effects, while absorption effects were taken into account only for compounds (**4**) and (**7**) using the empirical method of Walker and Stuart.[22] The structures were solved by Patterson (using the SHELX 86 program[23]) and Fourier techniques and refined on *F* by block-diagonal least squares (one block for the non-hydrogen atom parameters, the other for hydrogens when refined), using the SHELX 76 program.[24]

The analysis of complex (**7**) deserves some additional comments. During the refinement the Si(1) silylmethyl groups could not be located as no relevant peaks were found at a *R* value of 0.0761 that could not be further improved, clearly indicating the presence of disorder. At this point the positions of the methyls of this silyl group were calculated assuming a *trans* conformation, then the difference in potential energy was calculated for the different positions of the group by rotating it about the C(7)–Si(1) bond. The profile obtained is illustrated in Figure 6 which shows three minima corresponding to three possible orientations of the silyl group. Assuming these three orientations as equally probable, a trial model of disorder was considered assigning a occupancy factor of 0.33 for each orientation. Refinement of the structure according to this model, with no constraint on the atomic co-ordinates, immediately decreased the value of the *R* index, finally to 0.0593.

The hydrogen atoms were partly located from difference Fourier syntheses and partly placed in calculated positions and refined isotropically only in the case of compounds (**4**), (**5a**), and (**5b**).

The two crystallographically independent molecules present in the crystals of complex (**6**) are not significantly different. From PLUTO[25] drawings and the SYMMOL routine of PARST[26] it appears that the two molecules are related by a pseudo-two-fold screw axis running along *c* at $\approx\frac{1}{4}$ *a*, $\approx\frac{1}{4}$ *b*. The correctness of the space-group choice was checked by using TRACER,[27] NEWLAT,[28] and MISSYM[29] programs.

The atom–atom non-bonded potential-energy calculations were carried out with the ROTENER[20] program which makes use of a function of the type: $E_{ij} = B_{ij}\exp(-C_{ij}r_{ij}) - A_{ij}r_{ij}^{-6}$, disregarding the coulombic energy and assuming the H atoms to be in calculated positions (C–H 1.07).

Atomic scattering factors and anomalous scattering coefficients were taken from ref. 31. The calculations were carried out on the GOULD-SEL 32/77 computer of the Centro di Studio per la Strutturistica Diffrattometrica del CNR (Parma). In addition to the quoted programs, THMV[32] and ORTEP[33] were used.

Additional material available from the Cambridge Crystallographic Data Centre comprises H-atom co-ordinates, thermal parameters, and remaining bond distances and angles.

Acknowledgements

The authors are indebted to Professor C. Guastini (Parma) for collection of intensity data, and to the Centro CNR per lo Studio della Macromolecole Stereoordinate ed Otticamente attive (Pisa) for use of their n.m.r. facilities. Financial support from the Ministero della Pubblica Istruzione (Rome) and Consiglio Nazionale della Ricerche (CNR) (Rome) is gratefully acknowledged.

References

1 T. H. Tulip and T. H. Horn, *J. Am. Chem. Soc.*, 1981, **103**, 2448; R. A. Andersen, R. A. Jones, and G. Wilkinson, *J. Chem. Soc., Dalton Trans.*, 1978, 446; R. DiCosimo, S. S. Moore, A. F. Sowinski, and G. M. Whitesides, *J. Am. Chem. Soc.*, 1982, **104**, 124; J. W. Bruno, G. M. Smith, T. S. Marks, C. K. Fair, A. J. Schultz, and J. M. Williams, *ibid.*, 1986, **108**, 40.

2 G. W. Parshall, *Chem. Tech.*, 1984, 628; J-Y. Saillard and R. Hoffmann, *J. Am. Chem. Soc.*, 1984, **106**, 2006; R. H. Crabtree, *Chem. Rev.*, 1985, **85**, 245.

3 (*a*) P. Diversi, G. Ingrosso, A. Lucherini, and D. Fasce, *J. Chem. Soc., Chem. Commun.*, 1982, 945; (*b*) L. Andreucci, P. Diversi, G. Ingrosso, A. Lucherini, F. Marchetti, V. Adovasio, and M. Nardelli, *J. Chem. Soc., Dalton Trans.*, 1986, 477; (*c*) *ibid.*, p. 803.

4 P. Di Giorgio, P. Diversi, G. Ingrosso, A. Lucherini, F. Marchetti, V. Adovasio, and M. Nardelli, XIII International Conference on

Organometallic Chemistry, Torino, 4th—9th September, 1988, Abstracts, p. 442.

5 V. Schomaker and K. N. Trueblood, *Acta Crystallogr., Sect. B*, 1968, **24**, 63.

6 J. D. Dunitz and D. N. J. White, *Acta Crystallogr., Sect. A*, 1973, **29**, 93.

7 K. N. Trueblood, *Acta Crystallogr., Sect. A*, 1978, **34**, 950.

8 F. L. Hirshfeld, *Acta Crystallogr., Sect. A*, 1976, **32**, 239.

9 B. Rees and P. Coppens, *Acta Crystallogr., Sect. B*, 1973, **29**, 2515.

10 D. Cremer and J. A. Pople, *J. Am. Chem. Soc.*, 1975, **97**, 1354.

11 M. Nardelli, *Acta Crystallogr., Sect. C*, 1983, **39**, 1141.

12 R. Luck, R. H. Morris, and J. R. Sawyer, *Organometallics*, 1984, **3**, 1009.

13 M. A. Bennett, T-N. Huang, T. W. Matheson, and A. K. Smith, *Inorg. Synth.*, 1982, **21**, 74.

14 H. Werner and H. Kletzin, *J. Organomet. Chem.*, 1982, **228**, 289.

15 P. Barabotti, P. Diversi, G. Ingrosso, A. Lucherini, F. Marchetti, L. Sagramora, V. Adovasio, and M. Nardelli, *J. Chem. Soc., Dalton Trans.*, 1990, 179.

16 D. Seiferth and W. Freyer, *J. Org. Chem.*, 1961, **26**, 2604.

17 J. Ciabattoni, E. C. Nathan, A. E. Feiring, and P. J. Kocienski, *Org. Synth.*, 1974, **54**, 97.

18 J. W. Connolly and G. Urry, *Inorg. Chem.*, 1963, **2**, 645.

19 R. R. Schrock and J. D. Fellmann, *J. Am. Chem. Soc.*, 1978, **100**, 3359.

20 M. Nardelli and A. Mangia, *Ann. Chim. (Rome)*, 1984, **74**, 163.

21 J. B. Nelson and D. P. Riley, *Proc. Phys. Soc. (London)*, 1945, **57**, 160, 447.

22 N. Walker and D. Stuart, *Acta Crystallogr., Sect. A*, 1983, **39**, 158.

23 G. M. Sheldrick, SHELX 86, Program for Crystal Structure Solution, University of Göttingen, 1986.

24 G. M. Sheldrick, SHELX 76, Program for Crystal Structure Determination, University of Cambridge, 1976.

25 W. D. S. Motherwell and W. Clegg, PLUTO, University of Cambridge, 1976.

26 M. Nardelli, *Comput. Chem.*, 1983, **7**, 95.

27 S. L. Lawton and R. A. Jacobson, The Reduced Cell and its Crystallographic Applications, Ames Laboratory; available from the Clearing-house for Federal Scientific and Technical Information, National Bureau of Standards, U.S. Department of Commerce, Springfield, Virginia, 1965.

28 A. Mugnoli, *J. Appl. Crystallogr.*, 1985, **18**, 183.

29 Y. Le Page, *J. Appl. Crystallogr.*, 1987, **20**, 264.

30 M. Nardelli, ROTENER, a FORTRAN routine for calculating non-bonded potential energy, University of Parma, 1988.

31 'International Tables for *X*-Ray Crystallography,' Kynoch Press, Birmingham, 1974, vol. 4.

32 K. N. Trueblood, THMV, University of California, Los Angeles, 1984.

33 G. K. Johnson, ORTEP, Report ORNL 3794, Oak Ridge National Laboratory, Tennessee, 1965.

Received 10*th July* 1989; *Paper* 9/02889G